CORPUS PUBLISHERS

Current Trends in Engineering Science (CTES)

ISSN: 2833-356X

Volume 3 Issue 2, 2023

Article Information

Received date : April 06, 2023

Published date: May 01, 2023

*Corresponding author

Bright Bariakpoa Kinate, Department of Petroleum Engineering, Rivers State University, Nigeria

DOI: 10.54026/CTES/1026

Keywords

Relative Permeability; Hysteresis; Sequestration; Saline Aquifer; Trapped

Research Article

The Impact of Relative Permeability Hysteresis on CO2 Sequestration in Saline Aquifer

Nyelebuchi Amadichuku, Bright Bariakpoa Kinate*, Echeonwu Azubuike Isidore and Somiari Iyowuna Epelle

Department of Petroleum Engineering, Rivers State University, Nigeria

Abstract

This work analyzed the amount of capillary-trapped CO_2 for maximum residual gas saturation due to relative permeability hysteresis. Upward migration of CO_2 is unwanted because it increases the risk of CO_2 migration from storage sites to the surface. One way to mitigate CO_2 leakage risk is to reduce the vertical CO_2 migration to improved storage capacity and containment security. A compositional simulator (CMG-GEM) was used to simulate the flow of two components (CO_2 and H_2O). A fluid model was built with the PR 78 EOS using WINPROP. A base case model without relative permeability hysteresis was simulated and compared with the case with relative permeability hysteresis. The amount of CO_2 trapped, and CO_2 saturation distribution were analyzed for maximum trapped gas saturation of 0.3, 0.4 and 0.5. Results shows an increase in the amount of CO_2 trapped as the maximum residual gas saturation was increased from 0.3 to 0.4 and 0.5 with a value of 16560128mol for the base case study, 49041744mol, 59502924mol and 67286728mol respectively for maximum residual gas saturation due to relative permeability hysteresis of 0.3, 0.4 and 0.5 respectively. Very little accumulation of CO_2 occurs when the maximum trapped gas saturation due to relative permeability hysteresis was set at 0.5. Result reveals that after 200 years, almost all the CO_2 was trapped in the formation. Therefore, the imbibition cycle at the trailing end of the CO_2 plume should be considered as accounting for hysteresis effects has led to a spread-out distribution of trapped CO_2, as opposed to a concentrated distribution of mobile CO_2 without relative permeability hysteresis.

Introduction

There is little doubt that human socioeconomic activities has resulted to emissions of gas such as carbon(iv)oxide which has impacted negatively on the global carbon cycle [1]. The result of the release of CO_2 is an accumulation of carbon dioxide in the atmosphere, accompanied by a reduction in the pH of the upper ocean. The emission of carbon dioxide (CO_2), which is treated as one of the main reasons for global warming when fossil fuel is burned, cannot be avoided. Fossil-fueled power-production technology plays a significant role in contributing to the emission of greenhouse gases into the atmosphere. By reducing the emission of CO_2 into the atmosphere and by switching to an alternative power generation with zero-emission, it is possible to prevent future catastrophic effects. The carbon capture utilization and storage (CCUS) methods and technologies are among the many ways to reduce CO_2 emissions. CCUS technologies aim to capture CO_2 from large industrial sources and store it in underground structures or use it through conversion into useful products. Current predictions suggest that unless an aggressive reduction of net CO_2 emissions is implemented, carbon(iv)oxide concentrations in the atmosphere will continue to rise [2,3]. Since anthropogenic CO_2 emissions are primarily due to energy consumption and 85% of the primary power is supplied by fossil fuels, a drastic reduction in CO_2 emissions represents a major challenge [4]. CO_2 sequestration refers to the capture and long-term storage of anthropogenic CO_2 in order to limit its emission to the atmosphere [5]. Injection into geological formations is one option to store CO_2 [4,6,7]. Different target formations have been identified for this purpose, including depleted oil and gas reservoirs [8-10], unminable coal beds [11], and deep saline aquifers [12-15]. One of the major concerns in any sequestration project is the potential leakage of the CO_2 into the atmosphere. Possible causes of leaks are loss of integrity of the cap rock due to over pressurization of the geological formation [16,17], and abandoned wells that may be present [18]. When planning geologic sequestration projects in saline aquifers or depleted hydrocarbon reservoirs, it is therefore essential to predict the migration and distribution of the CO_2 in the subsurface structure so that injection can be maximized while keeping the risk of leakage at a minimum. Many authors have presented simulations of CO_2 injection and migration [19-27] using a variety of approaches. Because of the density difference between the CO_2 and the brine, the low viscosity CO_2 tends to migrate to the top of the geologic structure. This upward migration is sometimes delayed or suppressed by low permeability layers that impede the vertical flow of CO_2. Relative permeabilities are the key descriptors in classical formulations of multiphase flow in porous media. Experimental evidence and an analysis of pore-scale physics demonstrate conclusively that relative permeabilities are not single functions of fluid saturations and that they display strong hysteresis effects. Carbon(iv)oxide injection into depleted oil and gas fields represents a low-cost opportunity for CO_2 storage for many reasons including revenue from enhanced oil recovery and the ability to take advantage of existing reservoir characterization and site infrastructure. Understanding migration and trapping for CO_2 in these systems should be a high priority for research. The drainage and imbibition-like processes during the injection and post-injection stages of CO_2 storage led to hysteresis, a process where the capillary pressure and relative permeability curves change pathways. This phenomenon has been described as being very critical to the successful modeling of CO_2 trapping processes [28-30]. This is because as the CO_2 migrates upward after the injection phase, the remaining CO_2 plume gets disconnected due to water displacing CO_2 at the trailing edge and becomes a series of blobs. CO_2 is trapped in these blobs and the mechanism is termed residual or capillary trapping mechanism, which over time results in the dissolution of the CO_2 in the formation brine. Therefore, this work evaluates the relevance of relative permeability hysteresis when modelling geological CO_2 sequestration processes [31].

Methodology

Data and simulator model

The simulation tool and data used are; CMG pre-processor, Builder for writing GEM dataset, WINPROP fluid modelling package, GEM module of the CMG Builder for model validation and simulation runs, Rock physics functions (relative permeability, porosity and saturations), grid properties data (grid dimensions in the x, y and z directions, permeability of the grid cells in x, y and z directions, grid geometry, grid thickness, number of grid cells in the x, y and z directions and depth to the top of reservoir), fluid properties data (compositional analysis, brine properties), well data (trajectory and constraint, well type, injection fluid and composition etc). Grid properties data, relative permeability data, and model initialization data are shown in tables 1- 5.

Table 1: Grid properties data.

Properties	Value
Grid Top	1200m
Grid thickness	5m
Permeability (I, J and K)	100 millidarcies
Porosity	0.12
Rock compressibility	5.5e-7 per kPa
Reference pressure for rock compressibility	11800 kPa

Table 2: Data for GEM fluid model creation.

Component	Mole fraction
CH_4	0.999
CO_2	0.001
Reservoir temperature for GEM fluid model	50°C

Table 3: Water relative permeability data.

Sw	krw	krow
0.2	0	1
0.2899	0.0022	0.6769
0.3778	0.018	0.4153
0.4667	0.0607	0.2178
0.5558	0.1438	0.0835
0.6444	0.2809	0.0123
0.7	0.4089	0
0.7333	0.4855	0
0.8222	0.7709	0
0.9111	0.95	0
1	0.9999	0

Table 4: Gas relative permeability data.

Sg	krg	krog
0.0006	0	1
0.05	0	0.88
0.0889	0.001	0.7023
0.1778	0.01	0.4705
0.2667	0.03	0.2963
0.3556	0.05	0.1715
0.4444	0.1	0.0878
0.5333	0.2	0.037
0.6222	0.35	0.011
0.65	0.39	0
0.7111	0.56	0
0.8	0.9999	0

Table 5: Model initialization data.

Properties	Value
Temperature	50°C
Reference pressure	11800 kPa

Simulation process

CMG's GEM greenhouse gases (GEM GHG) option was applied to set up the base case simulation parameters. Builder was used for writing the dataset and was validated with CMG-GEM. A two-dimensional (2D) homogeneous aquifer model of dimension 100x1x20 (2000 grid blocks) in the x-, y- and z-directions and block width of 10ft both in the x- and y-directions was developed. The model was populated with petrophysical, grid and rock properties using the data in table 1. WINPROP was used to create a compositional fluid model required in the component section of CMG-GEM data file. A fluid model comprising of CO_2 and CH_4 in proportion of 0.001 and 0.999 was created in WINPROP using the PR 1978 EoS (Table 2). The CH_4 component was treated as the trace component. The created fluid model was imported into the component section of GEM data file. The data in tables 3 & 4 were used to define the relative permeability curves and the model was initialized using the data in table 5. Water-Gas contact was set at 1150m above the reference depth which gave a model fully saturated with brine. Gas cap was initialized with CO_2 fraction of 0.001 and CH_4 fraction of 0.999. An injector well 'CO_2_INJECTOR' was completed in three layers at the bottom of the model at 1298m, 1299m and 1300m. Pure supercritical CO_2 was injected into the aquifer at a maximum, constant surface gas rate of 10000m^3/day and maximum BHP of 44500kPa for 1 year. The injector was shut in, and the simulation period continues with only natural gradient/density differences driving the flow for the remaining 199years. Having established the base case model, sensitivity studies were conducted using the GEM keyword 'HYSKRG' to vary the maximum residual gas saturation. Land's model was used to evaluate the effect of hysteresis on CO_2 residual trapping performance. Three different maximum residual CO_2 saturations, 'HYSKRG' (0.3, 0.4 and 0.5) were considered.

Simulation workflow

The simulation workflow for this study is shown in figure 1.

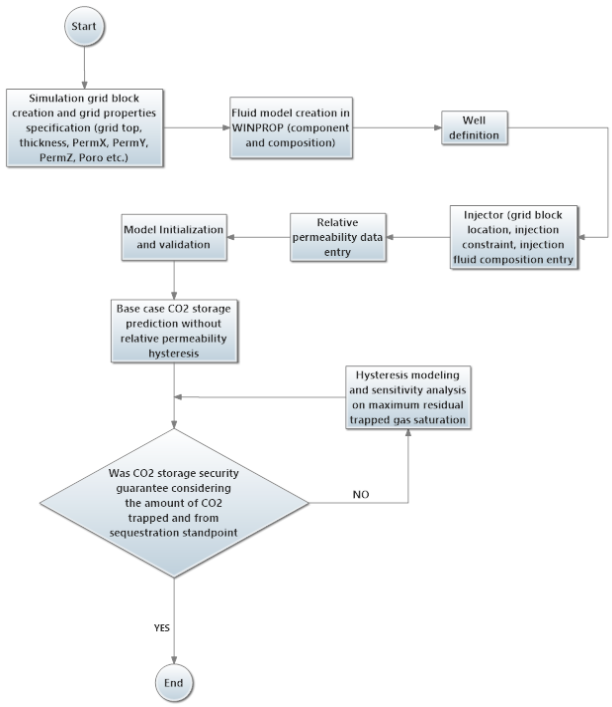

Figure 1: simulation work flow.

Results

Base case model without hysteresis

Figure 2 shows the CO_2 saturation distribution throughout the aquifer for the base case aquifer model without relative permeability hysteresis. The base case model simulates injection of CO_2 for 1-year, and the migration of the CO_2 plume by natural gradient during the next 199 years. Because the gas relative permeability is assumed to be irreversible (no hysteresis), the model does not predict any residual trapping of CO_2. The injected CO_2 in the model migrated laterally during the injection phase under the influence of pressure provided by the injection well (Figure 2). Post-injection, the lateral expansion of the plume ceased and CO_2 migrated upward due to lighter density of the CO_2 compared to formation water. The CO_2 plume migrates upward due to buoyancy forces without leaving any residual saturation behind.

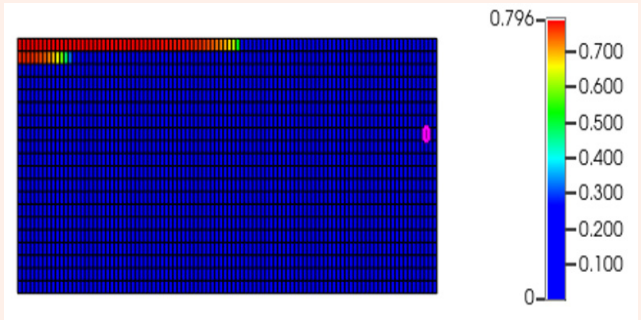

Figure 2: Upward migration of C CO_2 plume due to lighter density.

After a sufficiently long time (199years), the model predicts the formation of a gas cap of mobile CO_2 at the top of the formation. The plume travels through the formation without leaving any residual CO_2. This scenario is unfavourable from a sequestration standpoint: damage in the cap rock could lead to fractures that might serve as conduits for leaks of the mobile CO_2 to upper formations and eventually, the atmosphere. There was a higher gas saturation at the top of the structure ranging from 0.796 - 0.62 at the front of the CO_2 plume as seen in figure 3.

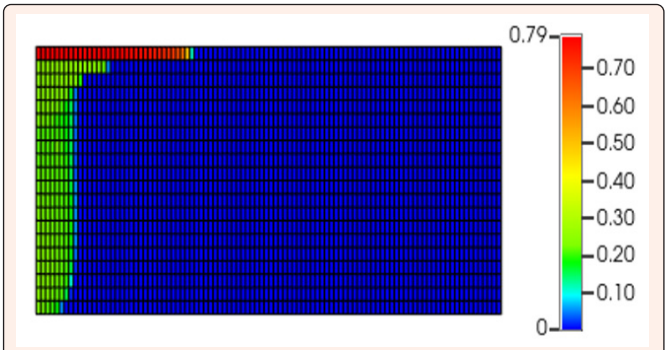

Figure 3: Gas (CO_2) saturation after 200years of injection.

Figure 4 shows the amount of CO_2 trapped after 200years for the base case run without accounting for relative permeability hysteresis. There was an increase in the amount of CO_2 trapped to 974635mol during the period of injection as the pressure from the injection well. Beyond this period, the amount of CO_2 trapped increases slightly as the plume migrate upward under the effect of natural buoyancy to 16560128mol for a period of 199years.

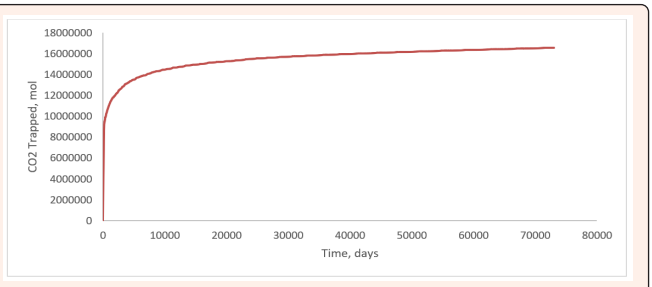

Figure 4: Amount of CO_2 trapped for the base case run after 200years.

Residual trapping

Maximum residual trapped gas saturation (HYSKRG = 0.3)

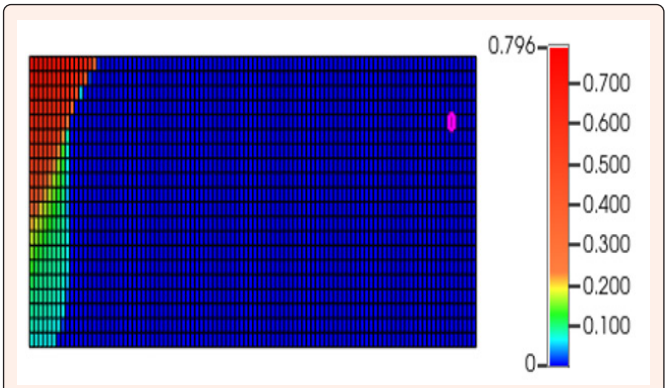

Figure 5: CO_2 saturation distribution at 200years for HYSKRG = 0.3.

Figure 5 shows the distribution of CO_2 saturation in the aquifer for the case in which relative permeability hysteresis was considered and maximum residual gas saturation of 0.3. After the injection phase, the model predicts a trail of residual, immobile CO_2 during the migration of the plume. Due to a net flow of CO_2 in the vertical direction, trapping prevents the injected CO_2 from forming a gas cap. There was a decrease in the amount of CO_2 reaching the top of the formation when compared with the case in which relative permeability hysteresis was not considered.

The amount of CO_2 trapped after 200years for the case with maximum trapped gas saturation due to relative permeability hysteresis of 0.3 is presented in figure 6. The amount of CO_2 trapped increases during the period of injection as the pressure from the injection well. During this period, 11916847mol of CO_2 was trapped. Beyond this period, the amount of CO_2 trapped increases slightly as the plume migrates upward under the effect of natural buoyancy to 49041744mol for a period of 199years.

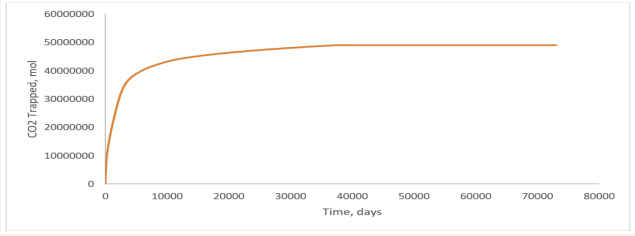

Figure 6: CO_2 trapped at 200years for HYSKRG=0.3.

Maximum residual trapped gas saturation (HYSKRG = 0.4)

The distribution of CO_2 saturation in the saline aquifer for the case in which relative permeability hysteresis was considered and at maximum residual gas saturation of 0.4 is presented in figure 7. After the injection phase, the model predicts a trail of residual, immobile CO_2 during the migration of the plume. There is a net flow of CO_2 in the vertical direction and residual trapping prevents the injected CO_2 from forming a large gas cap. A decrease in the amount of CO_2 reaching the top of the formation when compared with the case in which the maximum residual gas saturation due to relative permeability hysteresis was set at 0.3.

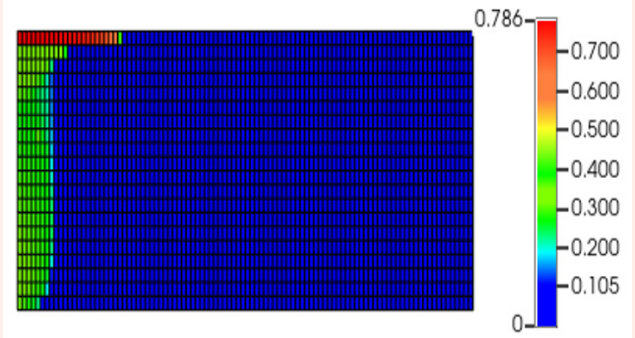

Figure 7: CO_2 saturation distribution at 200years for HYSKRG = 0.4.

The amount of CO_2 trapped after 200years for the case with maximum trapped gas saturation due to relative permeability hysteresis of 0.4 is shown in figure 8. Result shows an increase to 13618751mol of CO_2 trapped during the period of injection as the pressure from the injection well increases its migration into the pores of the surrounding formation. Beyond this period, the amount of CO_2 trapped increases slightly as the plume migrates upward under the effect of natural buoyancy to 59502924mol for a period of 199years.

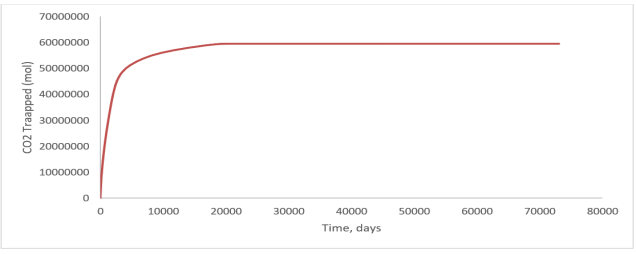

Figure 8: CO_2 trapped at 200years for HYSKRG=0.4.

Maximum residual trapped gas saturation (HYSKRG = 0.5)

Figure 9 shows the CO_2 saturation distribution in the saline aquifer for the case with maximum residual gas saturation due to relative permeability hysteresis of 0.5. In contrast to the case in which the maximum trapped gas saturation was set at 0.3 and 0.4 respectively, very little accumulation of CO_2 occurs when the maximum trapped gas saturation due to relative permeability hysteresis was set at 0.5. After 200 years, almost all the CO_2 was trapped in the formation. Accounting for hysteresis effects leads to a spread-out distribution of trapped CO_2, as opposed to a concentrated distribution of mobile CO_2. This scenario is more realistic and, importantly, much more favourable for the effectiveness of CO_2 sequestration as it minimizes the risk of leaks (the gas is immobile) and enhances other sequestration mechanisms such as dissolution into the brine and geochemical binding (more interfacial area between the CO_2 and the initial pore water).

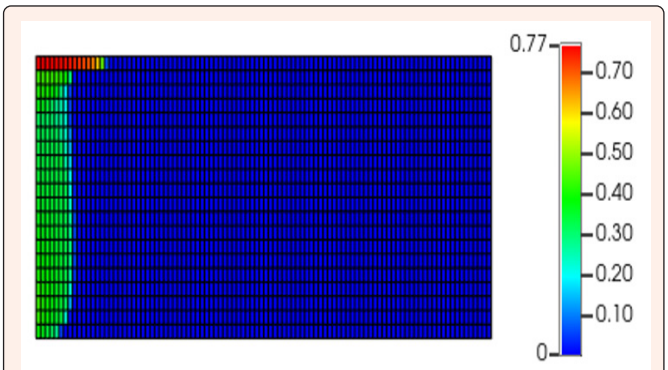

Figure 9: CO_2 saturation distribution at 200years for HYSKRG = 0.5.

The amount of CO_2 trapped after 200years for the case with maximum trapped gas saturation due to relative permeability hysteresis of 0.5 is shown in figure 10. There was an increase in the amount of CO_2 trapped to 974635mol during the period of injection as the pressure from the injection well. The amount of CO_2 trapped increases slightly as the plume migrates upward under the effect of natural buoyancy to 16560128mol for a period of 199years.

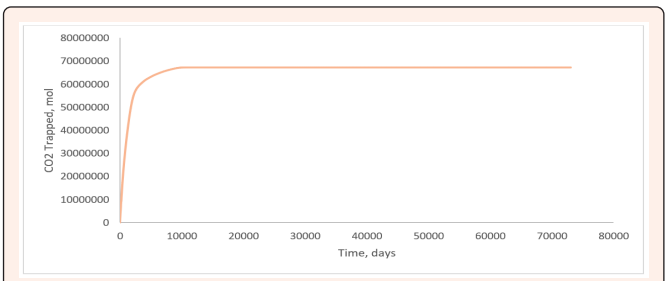

Figure 10: CO_2 trapped at 200years for HYSKRG=0.5.

Comparison of base case and relative permeability hysteresis cases

A higher amount of residual trapped CO_2 was obtained for case with relative permeability hysteresis structural trapping model than base case without relative permeability hysteresis. Figure 11 shows the extent of residual CO_2 trapping for the models with relative permeability hysteresis in comparison with only natural gradient. There is an increase in the amount of CO_2 trapped as the maximum residual gas saturation was increased from 0.3 to 0.4 and 0.5 with a value of 16560128 mol for the base case,49041744mol, 59502924- mol and 67286728mol for maximum residual gas saturation due to relative permeability hysteresis of 0.3, 0.4 and 0.5 respectively. There is an increase in the initial gas saturation before the start of the imbibition cycle at the trailing end of the CO_2 plume.

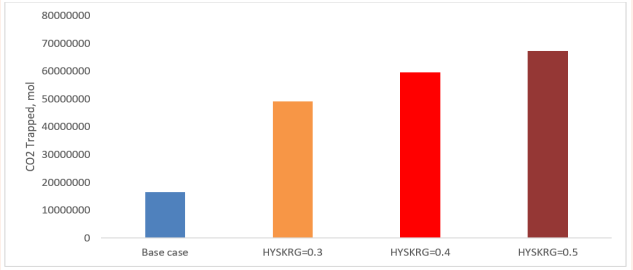

Figure 11: Comparison of CO_2 trapped for the base case and relative permeability hysteresis model.

Conclusion

This work investigated the impact of Relative Permeability Hysteresis and maximum residual gas saturation on storage performance of CO_2.
The following conclusions were drawn from this study:

a) The study confirms that trapping of CO_2 due to the effect of gas water relative permeability hysteresis can have a significant impact in the long-term success for a geosequestration project.

b) A significant residual trail of CO_2 remained around the wellbore as water imbibed behind the migrating plume. Thus, the impact of the mechanism of gas-water relative permeability hysteresis was verified.

c) There is a reduction in the amount of mobile CO_2 reaching the top of the structure as the maximum residual gas saturation increased

d) There is an increase in the amount of CO_2 trapped as the maximum residual gas saturation increased.

References

1. Falkowski P, Scholes RJ, Boyle EEA, Canadell J, Canfield D, et al. (2000) The global carbon cycle: A test of our knowledge of Earth as a system. Science 290(5490): 291-296.
2. Wigley TML, Richels R, Edmonds JA (1996) Economic and environmental choices in the stabilization of atmospheric CO_2 concentrations. Nature 379(6562): 240-243.
3. Hoffert MI, Caldeira K, Jain AK, Haites EF, Harvey LD, et al. (1998) Energy implications of future stabilization of atmospheric CO_2 content. Nature 395(6704): 881-884.
4. Orr FM (2004) Storage of carbon dioxide in geologic formations. Journal of Petroleum Technology. 56(9): 90-97.
5. Lackner KS (2003) A guide to CO_2 sequestration. Science 300(5626): 1677-1678.
6. Hitchon G, Gunter WD, Gentzis T, Bailey RT (1999) Sedimentary basins and greenhouse gases: A serendipitous association. Energy Conversion and Management 40(8): 825-843.
7. Bachu S (2000) Sequestration of CO_2 in geological media: Criteria and approach for site selection in response to climate change. Energy Conversion and Managemet 41(9): 953-970.
8. Holloway S (2001) Storage of fossil fuel-derived carbon dioxide beneath the surface of the earth. Annual Review of Energy and the Environment 26: 145-166.
9. Kovscek AR, Cakici MD (2005) Geologic storage of carbon dioxide and enhanced oil recovery. II. Co-optimization of storage and recovery. Energy Conversion and Management 46(11-12): 1941-1956.
10. Kovscek AR, Wang Y (2005) Geologic storage of carbon dioxide and enhanced oil recovery. I. Uncertainty quantification employing a streamline-based proxy for reservoir flow simulation. Energy Conversion and Management 46(11-12): 1920-1940.
11. Bromhal GS, Sams WN, Jikich S, Ertekin T, Smith DH (2005) Simulation of CO_2 sequestration in coal beds: The effects of sorption isotherms. Chemical Geology 217(3-4): 201-211.
12. Bruant RG, Celia MA, Guswa AJ, Peters CA (2002) Safe storage of CO_2 in deep saline aquifers. Environmental Science & Technology 36(11): 240-245.
13. Pruess K, Garcıa J (2002) Multiphase flow dynamics during CO2 disposal into saline Aquifers. Environmental Geology 42(2-3): 282-295.
14. Pruess K, Xu T, Apps J, Garcia J (2003) Numerical modelling of aquifer disposal of CO_2. Society of Petroleum Engineering Journal 8(1): 49-60.
15. Bachu S (2003) Screening and ranking of sedimentary basins for sequestration of CO_2 in geological media in response to climate change. Environmental Geology 44: 277-289.
16. Rutqvist J, Tsang CF (2002) A study of caprock hydromechanical changes associated with CO_2 injection into a brine formation. Environmental Geology 42(2-3): 296- 305.
17. Jimenez JA, Chalaturnyk RJ (2002) Integrity of bounding seals for geologic storage of greenhouse gases. SPE Pap. 78196, Society of Petroleum Engineers, Richardson, Texas, USA.
18. Nordbotten JM, Celia MA, Bachu S (2004) Analytical solutions for leakage rates through abandoned wells. Water Resources Research 40(4).
19. Ennis KJ, Paterson L (2002) Engineering aspects of geological sequestration of carbon dioxide. SPE Pap. 77809-MS, Society of Petroleum Engineers. Richardson, Texas, USA.
20. Wellman TP, Grigg RB, McPherson BJ, Svec RK, Lichtner PC (2003) The evaluation of CO2 – brine-rock interaction with laboratory flow test and reactive transport modelling. SPE/DOE International Symposium on Oilfield Chemistry, Houston, Texas, (SPE 80228).
21. Pruess K (2003) Numerical Simulation of Leakage from a Geologic Disposal Reservoir for CO_2, with Transitions between Super-and Sub-Critical Conditions, Lawrence Berkeley National Laboratory: Berkeley, CA, USA.
22. Xu TF, Apps JA, Pruess K (2003) Reactive geochemical transport simulation to study mineral trapping for CO_2 disposal in deep arenaceous formations. Journal Geophysical Research 108(B2): 2071.
23. Doughty C, Pruess K (2004) Modelling supercritical carbon dioxide injection in heterogeneous porous media. Vadose Zone Journal 3: 837-847.
24. Flett M, Gurton R, Taggart I (2004) The function of gas – water relative permeability hysteresis in the sequestration of carbon dioxide in saline formations. SPE Pap. 88485-MS. Society of Petroleum Engineers, Richardson, Texas, USA.
25. Kumar A, Ozah R, Noh M, Pope GA, Bryant S, et al. (2005) Reservoir simulation of CO_2 storage in deep saline aquifers. Society of Petroleum Engineering Journal 10(3): 336-348.
26. Mo S, Akervoll I (2005) Modelling long-term CO_2 storage in aquifer with a black-oil reservoir simulator. SPE Paper 93951-MS, Society of Petroleum Engineers, Richardson, Texas, USA.
27. Obi EOI, Blunt MJ (2006) Streamline-based simulation of carbon dioxide storage in a North Sea aquifer. Water Resouce Research 42(3).
28. Ghomian Y, Pope GA, Sepehrnoori K (2008) Hysteresis and field-scale optimization of WAG injection for coupled CO_2-EOR and sequestration. In: SPE symposium on improved oil recovery, Society of Petroleum Engineers.
29. Juanes R, Spiteri E, Orr FM, Blunt M (2006) Impact of relative permeability hysteresis on geological CO_2 storage. Water Resource Research 42(12).

30. Spiteri EJ, Juanes R, Blunt MJ, Orr FM (2005) Relative permeability hysteresis: Trapping models and application to geological CO_2 sequestration. In SPE Annual Technical Conference and Exhibition, Dallas, TX, (SPE 96448).

31. Godec M, Koperna G, Petrusak R, Oudinot A (2014) Enhanced gas recovery and CO_2 storage in gas shales: A summary review of its status and potential. Energy Procedia 63: 5849–5857.